Title

Methylamine Separations Enabled by Cooperative Ligand Insertion in Copper—Carboxylate Metal—Organic Frameworks

Journal

Journal of the American Chemical Society, 146(34)

ISSN

0002-7863

Authors

Graf, Katerina I

Huang, Adrian J

Meihaus, Katie R

et al.

Publication Date

2024-08-28

DOI

10.1021/jacs.4c06718

Peer reviewed

JACS
JOURNAL OF THE AMERICAN CHEMICAL SOCIETY
pubs.acs.org/JACS

Article

Methylamine Separations Enabled by Cooperative Ligand Insertion in Copper–Carboxylate Metal–Organic Frameworks

Katerina I. Graf, Adrian J. Huang, Katie R. Meihaus, and Jeffrey R. Long*

Cite This: J. Am. Chem. Soc. 2024, 146, 23943–23954

Read Online

ACCESS | Metrics & More | Article Recommendations | Supporting Information

ABSTRACT: Monomethylamine (NH_2CH_3), dimethylamine ($NH(CH_3)_2$), and trimethylamine ($N(CH_3)_3$) are important chemical feedstocks that are produced industrially as an azeotropic mixture and must be separated using an energy-intensive thermal distillation. While solid adsorbents have been proposed as alternatives to distillation for separating various industrial gas mixtures, methylamine separations remain largely unexplored in this context. Here, we investigate two isoreticular frameworks Cu(cyhdc) ($cyhdc^{2-}$ = *trans*-1,4-cyclohexanedicarboxylate) and Cu(bdc) (bdc^{2-} = 1,4-benzenedicarboxylate) as prospective candidates for this challenging separation, motivated by the recent discovery that Cu(cyhdc) reversibly captures ammonia through a unique framework-to-coordination polymer phase change. Through a combination of gas adsorption and powder X-ray diffraction analyses, we find that Cu(cyhdc) and Cu(bdc) reversibly bind large quantities of mono- and dimethylamine through framework-to-coordination polymer phase change mechanisms, although both frameworks adsorb only moderate amounts of trimethylamine via physisorption. Single-crystal X-ray diffraction analysis of select mono- and dimethylamine containing phases suggests that the number of hydrogen bond donors available and the linker donor strength are key factors influencing amine uptake. Finally, investigation of the tricomponent adsorption behavior of both materials reveals that Cu(cyhdc) is selective for the capture of monomethylamine from a range of mono-, di-, and trimethylamine mixtures.

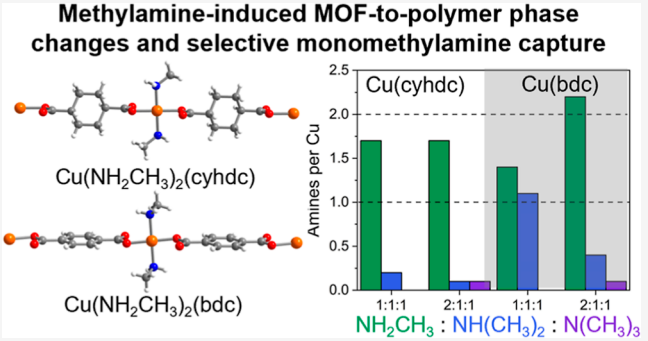

INTRODUCTION

Industrial chemical separations—many of which rely on energy-intensive distillation processes—account for at least 10% of global energy consumption.[1] In a greater push to reduce our dependence on fossil fuels, there is interest in the development of alternative methods that can replace distillation for numerous challenging separations in industry.[2] One such separation is the purification of mono-, di-, and trimethylamine produced from the reaction of ammonia and methanol.[3−9] These three amines are generated globally on a megaton scale every year,[3,4] and the demand for dimethylamine is particularly high.[3] The presence of trimethylamine in the final product mixture creates an azeotrope, increasing the complexity of at-scale separation.[8,9] Current industrial production requires four or more distillation columns to achieve 99% amine purity.[3]

A limited number of studies have explored the use of solid adsorbents for methylamine capture.[10−13] Recent work has investigated zeolites[10] or layered double hydroxides[11] for the removal of dimethylamine as a contaminant in waste and drinking water. Additionally, research in the 1970s investigated siliceous adsorbents for capturing gaseous mono-[12] as well as di- and trimethylamine[13] and found that the amines bind in the materials via weak physisorptive interactions. To our knowledge, however, no one has yet investigated the use of solid adsorbents for the separation of gaseous methylamines.

One class of adsorbents that has been extensively studied for the separation of industrially relevant chemicals are metal–organic frameworks (MOFs). Consisting of metal ions or cluster nodes connected by organic linkers, these crystalline, highly tunable porous solids have been designed to capture guest molecules via mechanisms involving coordinatively unsaturated metal sites[14,15] and pore-size dependent sieving,[16,17] among others.[18−21] For example, recent work from our laboratory showed that the Cu_2 paddlewheel-based framework Cu(cyhdc) ($cyhdc^{2-}$ = *trans*-1,4-cyclohexanedicarboxylate; Figure 1a)[22,23] selectively and reversibly captures up to four equivalents of ammonia per copper(II) center through a unique cooperative ligand insertion mechanism that results in the formation of one-dimensional $Cu(NH_3)_4(cyhdc)$ chains.[24]

Received: May 17, 2024
Revised: August 7, 2024
Accepted: August 8, 2024
Published: August 16, 2024

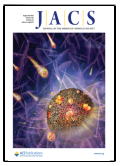

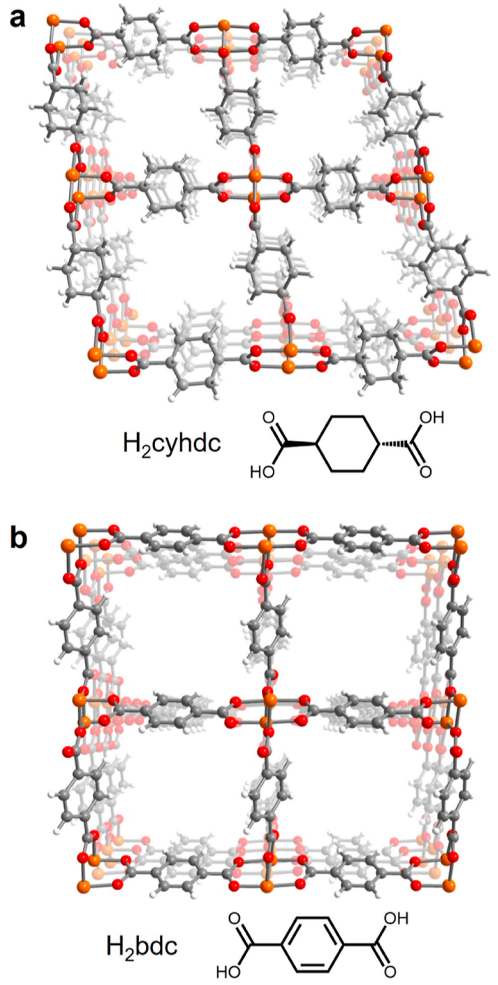

Figure 1. Illustration of the structures of (a) Cu(cyhdc) and (b) Cu(bdc) and their corresponding linkers. The vertices in each structure are formed by Cu−carboxylate paddlewheel units, and the one-dimensional channels run along the *a* direction.[22,29] Orange, red, gray, and white spheres represent Cu, O, C, and H atoms, respectively.

Primary- and secondary-sphere hydrogen bonding interactions between coordinated ammonia and carboxylate linkers provide stability to this structure and are thought to contribute significantly to the driving force for the unique phase change. Ammonia uptake in this system is reversible, and regeneration of Cu(cyhdc) occurs by way of an intermediate one-dimensional solid, $Cu(NH_3)_2$(cyhdc).

Other recent reports of copper(II)−carboxylate frameworks exhibiting high NH_3 capacities,[25−27] including Cu(bdc) (bdc^{2-} = 1,4-benzenedicarboxylate),[23,28,29] suggest that this class of materials may be candidates for the capture and/or separation of other strongly binding amines. Considering this, we were interested in the prospect of using copper(II)−carboxylate frameworks for the selective separation of mixtures of mono-, di-, and trimethylamine. We hypothesized that monomethylamine (NH_2CH_3) would selectively react with Cu(cyhdc) to stabilize a phase change similar to that observed with NH_3, while a phase change triggered by amine insertion would be less favorable with more substituted dimethylamine ($NH(CH_3)_2$) and trimethylamine ($N(CH_3)_3$). Further, selectivity would likely be dictated by sterics, the relative σ-donor strengths of the amines versus the dicarboxylate linker,[24] and the extent of any hydrogen bonding networks formed in the new phases.

Here, we report our investigation of the methylamine adsorption properties of Cu(cyhdc) and isoreticular Cu(bdc)—which features weaker copper−oxygen bonds (Figure 1b)—using isothermal adsorption and single crystal and powder X-ray diffraction analyses. While trimethylamine uptake in both materials occurs via physisorption, uptake of mono- or dimethylamine can trigger phase changes to one- or two-dimensional solids, depending on the identity of the amine. Preliminary multicomponent adsorption analyses indicate that as a result of its distinct methylamine adsorption properties, Cu(cyhdc) can selectively remove monomethylamine from mixtures with di- and trimethylamine at a range of partial pressures.

RESULTS AND DISCUSSION

Synthesis and Amine Adsorption Properties. The frameworks Cu(cyhdc) and Cu(bdc) were synthesized using a modified version of reported procedures (see the Experimental Section and Figures S1 and S2).[22,24,28] Both frameworks feature one-dimensional channels with dicopper paddlewheel nodes running along the *a* direction, which are bridged by dicarboxylate linkers to form rhombic (Cu(cyhdc)) or square (Cu(bdc)) channels (Figure 1). Powder X-ray diffraction data collected for activated microcrystalline samples of both materials are consistent with predicted patterns generated from their reported structures (Figure S1, Tables S2 and S3).[22,29] Brunauer−Emmett−Teller (Langmuir) surface areas of 381 and 729 m^2/g (430 and 802 m^2/g) were determined for Cu(cyhdc) and Cu(bdc), respectively, based on N_2 adsorption data collected at 77 K (Figure S2), and these values are consistent with prior reports.[23,29]

Isothermal mono-, di-, and trimethylamine adsorption and desorption data were collected for both materials at 25 °C and pressures ranging from 0 to 1 bar (Figure 2). Note: these amines are corrosive, flammable, and toxic gases that must be handled in a fume hood with all proper precautions (see the Experimental Section for details). Steep uptake of monomethylamine in Cu(cyhdc) occurs at 10 mbar, and the material achieves a capacity of 8.0 mmol/g at 36 mbar (Figure 2a, yellow data), consistent with the expected uptake for the adsorption of two amines per copper center (8.1 mmol/g). At higher pressures, the uptake levels off, reaching 9.4 mmol/g at 1 bar. The steep uptake and high capacity suggest that monomethylamine adsorption in Cu(cyhdc) may induce a structural phase change, analogous to that reported for NH_3.[24] Isothermal desorption of monomethylamine occurs with substantial hysteresis, and at 3.0 mbar the material retains a capacity of 8.8 mmol/g.

Uptake of dimethylamine in Cu(cyhdc) at 25 °C is less steep, although an inflection point is visible in the isotherm at ∼500 mbar (Figure 2a, orange data). At this pressure, the material achieves a capacity of 3.2 mmol/g, which corresponds to the uptake of approximately one amine per copper site. At 1 bar, the capacity is 5.6 mmol/g, close to that expected for adsorption of 1.5 equiv of dimethylamine per copper center (6 mmol/g). Interestingly, in dimethylamine adsorption data collected at 10 °C, there are two distinct step-like regions of gas uptake at ∼5 and 300 mbar (see Figure S3). After this steep uptake, the adsorption begins to plateau at capacities close to those expected for adsorption of one and two dimethylamines per copper site, respectively. This total uptake

https://doi.org/10.1021/jacs.4c06718
J. Am. Chem. Soc. 2024, 146, 23943−23954

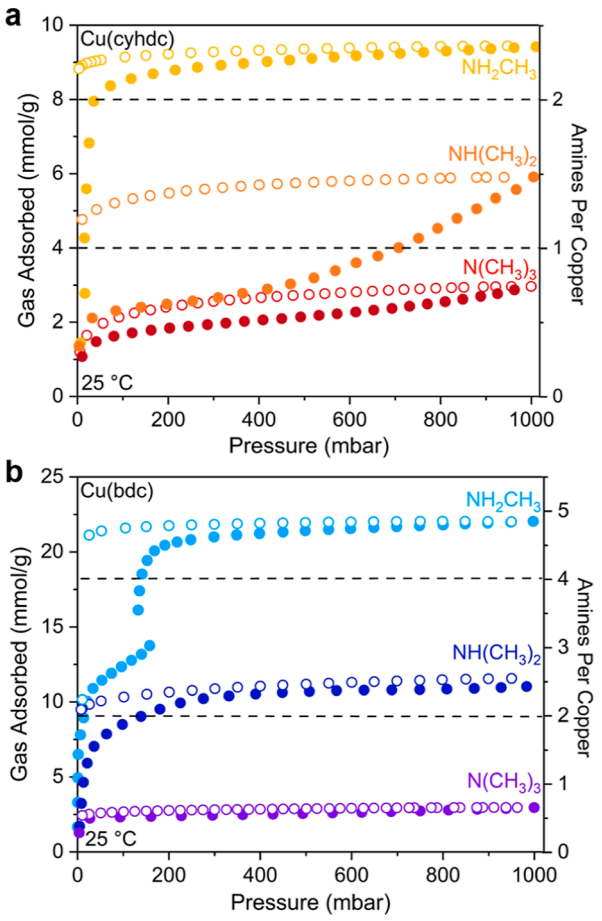

Figure 2. Pure mono-, di-, and trimethylamine adsorption and desorption isotherms (closed and open circles, respectively) collected at 25 °C for (a) Cu(cyhdc) and (b) Cu(bdc). Predicted amine uptakes corresponding to 1, 2, or 4 amines per copper site are shown as dashed lines.

is comparable with the uptake of monomethylamine at 25 °C and suggests that dimethylamine uptake in Cu(cyhdc) may also trigger a phase change, albeit one that is more favorable at lower temperatures. Dimethylamine desorption at 25 °C occurs with significant hysteresis, and the material retains 4.8 mmol/g of dimethylamine at 10 mbar. Finally, uptake of trimethylamine in Cu(cyhdc) is even less steep at 25 °C (Figure 2a, red data), and the material achieves a capacity of 2.9 mmol/g at 1 bar, less than the capacity that would be expected for adsorption of one trimethylamine per copper center (4 mmol/g). Desorption of trimethylamine under vacuum at 25 °C occurs with only a small amount of hysteresis, and 1.0 mmol/g of trimethylamine remained adsorbed in the material at the lowest accessible pressure of 10 mbar.

The methylamine adsorption data for Cu(bdc) generally follow a similar trend to that seen for Cu(cyhdc), in particular monomethylamine uptake was found to be the highest over the entire pressure range, followed by dimethylamine and trimethylamine (Figure 2b). Monomethylamine uptake occurs in two distinct steps, with onset pressures of ∼0.5 and 150 mbar, respectively, and the capacities in the poststep regions exceed those expected for the adsorption of two and four amines per copper (Figure 2b, light blue data). The first step occurs at a lower pressure than that associated with monomethylamine uptake in Cu(cyhdc), and the total gravimetric monomethylamine capacity at 1 bar is much higher than that determined for Cu(cyhdc), both of which results are consistent with the presence of weaker carboxylate donors in Cu(bdc). Isothermal desorption at 25 °C occurred with significant hysteresis, and the material retained a capacity of 10.2 mmol/g at 10 mbar, corresponding to two amines per copper site. Interestingly, the monomethylamine adsorption/desorption data are reminiscent of previously reported ammonia adsorption and desorption in Cu(cyhdc). This material adsorbs four ammonia molecules per copper site at 25 °C and 1 bar via a phase change to the one-dimensional solid $Cu(NH_3)_4$(cyhdc), while upon desorption, an intermediate chain structure is formed with only two ammonia molecules bound per copper site.[24]

Uptake of dimethylamine in Cu(bdc) occurs in a steep fashion at low pressures and begins to level off above 50 mbar, reaching a value of 11.0 mmol/g at 1 bar (Figure 2b, dark blue data) that is slightly higher than the predicted uptake assuming adsorption of two amines per copper site (8.8 mmol/g). Isothermal dimethylamine desorption data revealed that this uptake is largely irreversible at 25 °C, and the material retains 9.5 mmol/g at 7.7 mbar. However, consistent with the results obtained for Cu(cyhdc), the dimethylamine adsorption behavior at 10 °C is markedly different, and Cu(bdc) achieves a higher overall capacity and exhibits more clearly defined regions of sharp uptake, with capacities close to those predicted for adsorption of two and three amines per copper site, respectively (Figure S4). Isothermal adsorption data collected at higher temperatures for mono- and dimethylamine adsorption in Cu(bdc) and Cu(cyhdc) indicate that the uptake of these gases (and any corresponding structural changes) is strongly dependent on temperature; however, in the subsequent discussion, we focus on the methylamine adsorption properties of both materials only at ambient temperature. Finally, analogous to what was seen for Cu(cyhdc), Cu(bdc) adsorbs relatively little trimethylamine and without any regions of steep uptake, achieving a capacity of 3.0 mmol/g at 1 bar and 25 °C (Figure 2b, purple data). Desorption occurs with some hysteresis, and at 10 mbar a capacity of 2.5 mmol/is retained.

Powder X-ray Diffraction Analysis. As an initial probe of phase changes occurring upon methylamine uptake in Cu(cyhdc) and Cu(bdc), we collected powder X-ray diffraction data for samples of both materials before and after ex situ dosing with mono-, di-, or trimethylamine (see the Experimental Section for details). In brief, activated Cu(cyhdc) or Cu(bdc) was dosed with 1 bar of gas at 25 °C and allowed to equilibrate for 1 day before being brought into a N_2 glovebox for handling and analysis. Fourier transform infrared spectra collected for the mono- and dimethylamine dosed samples feature characteristic N−H and C−H stretches between 2750 and 3250 cm^{-1}, while weak C−H stretches are also apparent in spectra obtained for the materials dosed with trimethylamine (Figure S8). Proton NMR spectroscopy analysis of acid-digested samples revealed mono- and dimethylamine loadings consistent with those determined from gas adsorption analysis at 1 bar. The loading of trimethylamine, however, was significantly lower (Table S1), which we attribute to off-gassing of weakly physisorbed trimethylamine from the sample. Similar loadings were estimated from thermogravimetric analysis data collected for the amine-dosed samples under flowing N_2 (Figure S5 and Table S1).

https://doi.org/10.1021/jacs.4c06718
J. Am. Chem. Soc. 2024, 146, 23943−23954

Powder X-ray diffraction patterns collected for samples of Cu(cyhdc) and Cu(bdc) dosed with trimethylamine are indistinguishable from those of the bare frameworks, and unit cell parameters obtained from Pawley refinements of the data are the same as those of the parent materials (Tables S2 and S3), indicating that under these conditions, trimethylamine uptake does not induce a phase change. In contrast, exposure of Cu(cyhdc) to 1 bar of NH_2CH_3 at 25 °C for 1 day resulted in the formation of a new phase (Figure 3a; Table S1)

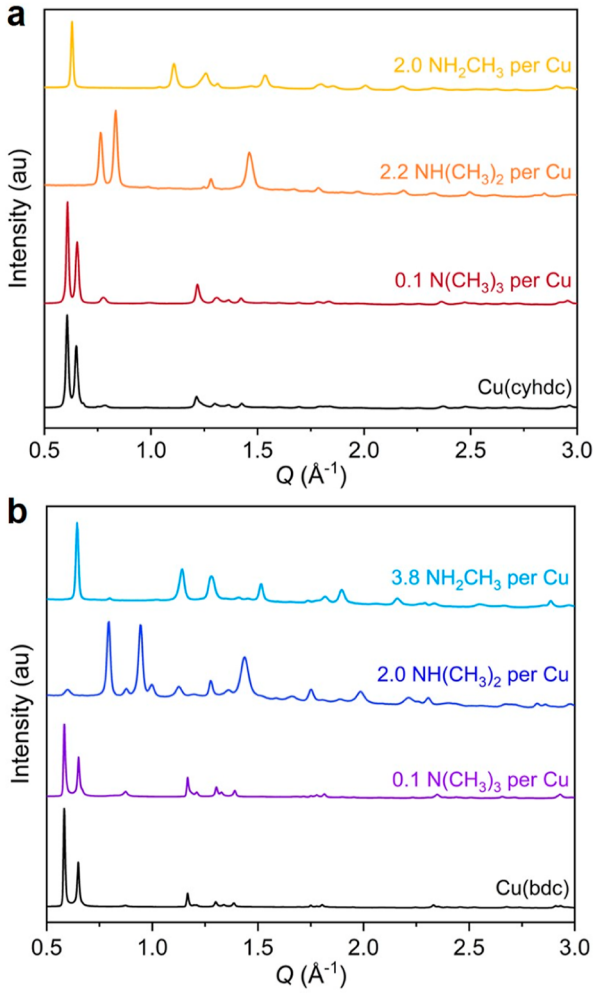

Figure 3. Synchrotron powder X-ray diffraction patterns (λ = 0.45171 or 0.1814 Å) collected at room temperature for samples of (a) Cu(cyhdc) and (b) Cu(bdc) before and after dosing with mono-, di-, or trimethylamine at 1 bar and 25 °C (10 °C in the case of Cu(cyhdc) and dimethylamine). Samples were equilibrated for 1 day under the dosing conditions before analysis (see the Experimental Section for details). Pawley refinement details for all the patterns are given in Tables S2 and S3. Amine loadings for the gas-dosed samples were determined from ^{1}H NMR spectroscopy analysis of acid-digested samples (see Table S1, see the Experimental Section for details).

with approximately two amines per copper that could be indexed with a $P\bar{1}$ unit cell, hereafter $Cu(NH_2CH_3)_2$(cyhdc) (Table S2). The solid also underwent a distinct color change from blue to purple after amine dosing, indicative of a change in the copper coordination environment. Interestingly, a powder pattern obtained for this sample after sitting for 3 weeks revealed the formation of a different phase with a higher symmetry space group ($C2/c$ versus $P\bar{1}$; see Figure S24 and Table S2). Powder X-ray diffraction data collected for samples of Cu(cyhdc) dosed ex situ with low pressures of monomethylamine—corresponding to those associated with the steep uptake region in the adsorption data—indicate that the formation of the $P\bar{1}$ phase begins to occur at gas pressures as low as 20 mbar and is complete at around 40 mbar (see Figure S10).

Powder X-ray diffraction data obtained for Cu(cyhdc) dosed with ∼1 bar of dimethylamine at 25 °C after 1 day also feature new reflections indicative of the formation of a new phase (Figure S9), and the color of the solid was observed to change from a teal blue to darker blue upon dosing. This transition occurs slower than that triggered by monomethylamine, however, and diffraction peaks for bare Cu(cyhdc) persisted even after the sample had equilibrated for 5 days. In contrast, dosing Cu(cyhdc) with 1 bar dimethylamine at 10 °C and allowing the sample to equilibrate for 1 day at this temperature resulted in a more rapid and complete transition to the new phase, which features two amines per copper center, hereafter $Cu(NH_2(CH_3)_2)_2$(cyhdc) (see Tables S1 and S2 and Figure 3a). The temperature dependence of the dimethylamine-induced phase change is consistent with the isothermal dimethylamine adsorption data discussed above; indeed, at 25 °C, dimethylamine uptake is not steep, and less than two amines are adsorbed per copper site. In contrast, at 10 °C, there are more clearly defined step regions, consistent with a phase change, and the uptake at 1 bar corresponds to approximately two amines per copper. The new diffraction pattern was refined with a $P\bar{1}$ unit cell, with different parameters than those obtained upon dosing with monomethylamine (Table S2). This phase was found to persist after storage for 3 weeks at 25 °C, in contrast to what was observed for the monomethylamine-dosed Cu(cyhdc) sample.

Dosing Cu(bdc) with 1 bar of mono- or dimethylamine at 25 °C resulted in the formation of new phases after 1 day (Figure 3b), which were assigned as $Cu(NH_2CH_3)_4$(bdc) and $Cu(NH_2(CH_3)_2)_2$(bdc), respectively, based on ^{1}H NMR spectra collected for acid digested samples (Table S1). Pawley refinement of diffraction data revealed that these phases form in the space groups $P\bar{1}$ and $P2_1/c$, respectively (Table S3). Diffraction data collected for Cu(bdc) dosed with low pressures of monomethylamine suggest that the transition to the $P\bar{1}$ phase is more complex than the phase change triggered by monomethylamine adsorption in Cu(cyhdc) (see Figure S11). For example, the formation of a new phase was apparent in the diffraction pattern collected for a sample of Cu(bdc) equilibrated with just 5 mbar of monomethylamine, while a sample equilibrated with 40 mbar of the gas (corresponding to just after the first steep uptake region in Figure 2b) was amorphous. Equilibration of Cu(bdc) with 100 mbar of monomethylamine resulted in an intermediate crystalline phase assigned as $Cu(NH_2CH_3)_2$(bdc) (based on ^{1}H NMR spectroscopy analysis of a digested sample; space group $P2_1/c$). Diffraction data collected for Cu(bdc) dosed with low pressures of dimethylamine suggest that the phase change to $Cu(NH_2(CH_3)_2)_2$(bdc) also occurs by way of an amorphous intermediate (Figure S11).

Powder X-ray diffraction data were also collected to explore the reversibility of the methylamine-induced phase changes. Samples of $Cu(NH_2CH_3)_2$(cyhdc), $Cu(NH_2(CH_3)_2)_2$(cyhdc), $Cu(NH_2CH_3)_4$(bdc), and $Cu(NH_2(CH_3)_2)_2$(bdc) were generated by dosing the parent frameworks with ∼1 bar of mono- or dimethylamine at 25 or 10 °C, as described above. In situ

https://doi.org/10.1021/jacs.4c06718
J. Am. Chem. Soc. 2024, 146, 23943−23954

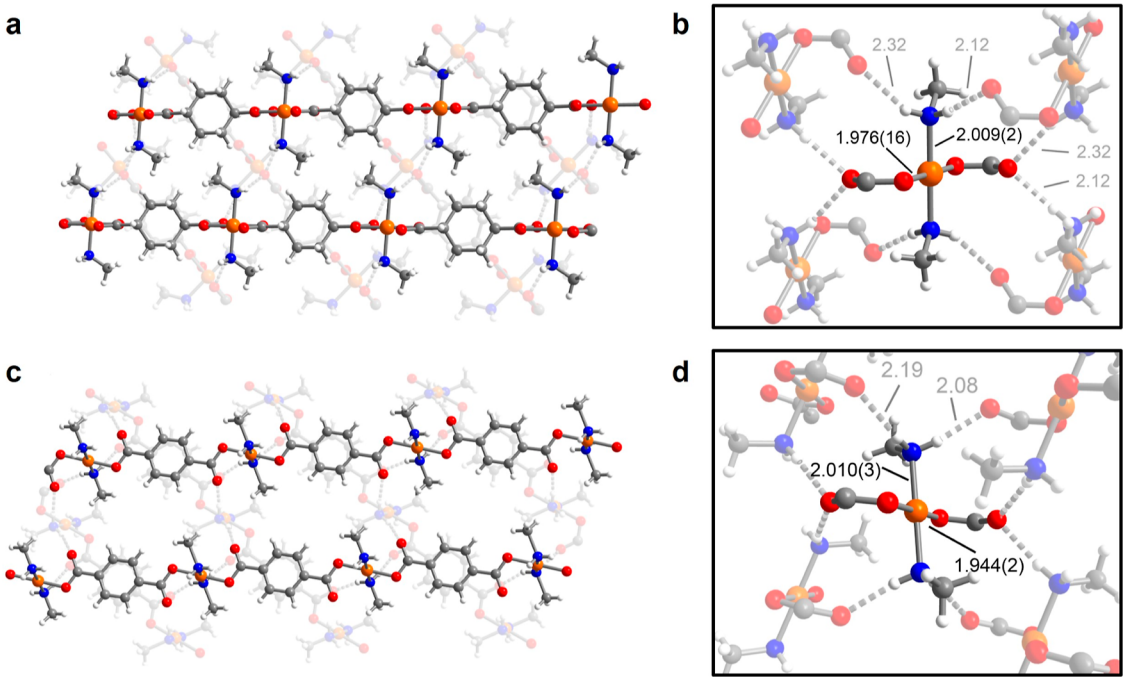

Figure 4. (a) Illustration of the $Cu(NH_2CH_3)_2(cyhdc)$ structure determined from X-ray diffraction analysis. This structure corresponds to that formed after dosing Cu(cyhdc) with 1 bar of monomethylamine and equilibration of the resulting sample for 3 weeks (see Figure S24). (b) Expanded view of the local copper coordination environment in $Cu(NH_2CH_3)_2(cyhdc)$, with selected Cu−linker and hydrogen bond distances given in Å. (c) Illustration of the $Cu(NH_2CH_3)_2(bdc)$ structure determined from X-ray diffraction analysis. This structure corresponds to the crystalline phase formed after dosing Cu(bdc) with monomethylamine and equilibration to a final monomethylamine pressure of 200 mbar (see Figure S25). (d) Expanded view of the local copper coordination environment in $Cu(NH_2CH_3)_2(bdc)$, with selected Cu−linker and hydrogen bond distances given in Å. Orange, red, blue, gray, and white spheres represent Cu, O, N, C, and H atoms, respectively. Hydrogen bonds are indicated with dashed lines.

diffraction data were then collected while heating the samples under flowing N_2 (Figures S12 and S13). It was possible to regenerate Cu(cyhdc) upon heating $Cu(NH_2CH_3)_2(cyhdc)$ or $Cu(NH_2(CH_3)_2)_2(cyhdc)$ to 175 or 185 °C, with the onset of the phase transitions starting as low as ∼145 or ∼125 °C (Figure S12). These temperatures are consistent with those associated with the onset of initial mass loss in thermogravimetric analysis data collected for the methylamine phases under flowing N_2 (Figure S5). In contrast, heating $Cu(NH_2CH_3)_4(bdc)$ or $Cu(NH_2(CH_3)_2)_2(bdc)$ as high as 200 °C under flowing N_2 resulted in the formation of amorphous phases (Figure S13). However, based on additional diffraction data collected for Cu(cyhdc) and Cu(bdc) after (i) dosing with mono- or dimethylamine at 1 bar and 25 or 10 °C, (ii) heating at 180 °C under flowing N_2, and (iii) dosing again with the respective amines, the crystalline methylamine-containing phases can be reformed after one adsorption and desorption cycle (see Figures S14 and S15 for details; in the case of Cu(bdc) and NH_2CH_3, a second unknown phase is also formed).

In order to further explore the stability of the methylamine-induced phase changes, extended methylamine adsorption−desorption cycling data were collected for Cu(cyhdc) and Cu(bdc) by dosing with mono- or dimethylamine at 1 bar and 25 or 10 °C and then heating under flowing N_2 using a thermogravimetric analyzer, which allowed for determination of the quantity of adsorbed amine. For both frameworks, relatively stable and high amine capacities were retained over the course of five adsorption−desorption cycles (see Figures S16−S23 and Table S4). In the case of Cu(bdc), it was not possible to regenerate the original framework upon final desorption of monomethylamine or dimethylamine after cycling, consistent with the preliminary powder X-ray diffraction cycling data described above. However, approximately four and two mono- and dimethylamines per copper were captured by the sample during each adsorption run, consistent with the capacity expected based on our isothermal adsorption data. Further, after the final desorption run, it was possible to regenerate the expected $Cu(NH_2CH_3)_4(bdc)$ and $Cu(NH(CH_3)_2)_2(bdc)$ phases after redosing with 1 bar of the respective amines (see Figures S20−S23).

In the case of the monomethylamine cycling data collected for Cu(cyhdc), the amine loading calculated from the desorption traces was ∼2 NH_2CH_3/Cu, after accounting for additional amine loading likely due to physisorption (see Figure S16 and Table S4). This value is consistent with that expected based on the isothermal adsorption data, and powder X-ray diffraction characterization of the solid sample after the fifth desorption run revealed that Cu(cyhdc) was regenerated with high crystallinity (Figure S17). Interestingly, however, dosing this regenerated sample again with 1 bar of monomethylamine yielded a solid with a powder X-ray diffraction pattern corresponding to the higher symmetry $C2/c$ $Cu(NH_2CH_3)_2(cyhdc)$ phase formed after initial dosing with monomethylamine followed by 3 weeks of equilibration, rather than the $P\bar{1}$ phase formed after dosing with 1 bar of amine and 1 day of equilibration (see Figure 3). The cycling data were collected over the course of approximately 3 days, and therefore equilibration times much shorter than 3 weeks are apparently sufficient to form the higher-symmetry phase.

The dimethylamine cycling results for Cu(cyhdc) are somewhat unusual. In particular, the desorption traces

https://doi.org/10.1021/jacs.4c06718
J. Am. Chem. Soc. 2024, 146, 23943−23954

consistently feature two steps at ∼50 and ∼125 °C, corresponding to the loss of ∼1 and ∼2 amines per copper, respectively (Figure S18, Table S4) and an overall loading of three amines per copper upon dimethylamine uptake at 1 bar and 10 °C. Notably, this is distinct from the results of the isothermal adsorption and powder X-ray diffraction data discussed above, which indicated that only two amines are bound per copper center when the parent framework is dosed at 10 °C for 1 day (Figures 2 and 3). After the fifth cycle, it was possible to regenerate Cu(cyhdc) based on powder X-ray diffraction analysis (see Figure S19), although the corresponding peaks are very broad, indicating that the particle size is small. Powder X-ray diffraction analysis of this sample after dosing again with 1 bar of dimethylamine at 10 °C for 1 day revealed a new crystalline phase (Figure S19), likely corresponding to the unknown $Cu(NH(CH_3)_2)_3$(cyhdc) phase consistently formed over the course of cycling. This result is currently not understood, although it is hypothesized to be a consequence of the different framework sample size and dosing conditions used in the cycling experiment relative to those for collecting isothermal adsorption and powder X-ray diffraction data shown in Figures 2 and 3 (refer to the Experimental Section for details). Ultimately, our cycling results indicate that relatively stable mono- and dimethylamine cycling capacities can be achieved with both frameworks.

Single-Crystal X-ray Diffraction Analysis. We sought to grow single crystals of the new methylamine-containing phases formed upon dosing with 1 bar of mono- or dimethylamine, motivated by an analogous approach that was previously successful for isolating single crystals of the $Cu(NH_3)_2$(cyhdc) and $Cu(NH_3)_4$(cyhdc) phases generated upon dosing Cu(cyhdc) with ammonia.[24] To this end, solutions of copper(II) triflate in *N*,*N*-dimethylformamide or ethanol were combined with a solution of excess linker and the desired amine in methanol or ethanol, and each mixture was placed inside a larger vial containing *N*,*N*-dimethylformamide (see the Experimental Section for details). After 1 day of vapor diffusion, purple and blue crystals had grown from the monomethylamine and dimethylamine solutions, respectively.

Crystals grown from the solution of copper(II), monomethylamine, and H_2cyhdc correspond to the one-dimensional phase $Cu(NH_2CH_3)_2$(cyhdc) (space group *C*2/*c*) formed after equilibration of Cu(cyhdc) with monomethylamine gas for 3 weeks (Figures 4a and S24). The structure of $Cu(NH_2CH_3)_2$(cyhdc) consists of chains of square planar copper centers coordinated by two *trans* monomethylamine ligands and bridged by *trans* cyhdc^{2-} linkers coordinated via a single oxygen. The structure of the individual chains is analogous to that reported for $Cu(NH_3)_2$(cyhdc) (space group $P\bar{1}$),[24] although the chains pack differently in three-dimensional space. Monomethylamines in adjacent $Cu(NH_2CH_3)_2$(cyhdc) chains engage in interchain hydrogen bonding interactions with the noncoordinated oxygen atoms of each linker (distances of 2.12 and 2.32 Å) (Figure 4b). This structure is consistent with the isothermal NH_2CH_3 adsorption data obtained at 25 °C, which revealed steep uptake of ∼2 amines per copper site (Figure 2a). While the structure of the $Cu(NH_2CH_3)_2$(cyhdc) phase formed directly after dosing with monomethylamine is unknown, we hypothesize that this phase also features one-dimensional chains with two NH_2CH_3 coordinated to each copper, but has a different packing of the chains. It is possible that a longer period of equilibration with the gas (e.g., 3 weeks versus 1 day, see Figure S24) allows for a rearrangement to the *C*2/*c* phase. The methanol and/or *N*,*N*-dimethylformamide in the crystallization solution may support the direct formation of this higher symmetry phase, by engaging in hydrogen bonding interactions with structural fragments formed in solution.

Efforts to grow crystals of the phase formed after equilibration of Cu(cyhdc) to 1 bar of dimethylamine at 10 °C were unsuccessful (Figures 3a and S24). However, from a solution of copper(II), H_2cyhdc, and dimethylamine, we were able to isolate crystals of a one-dimensional compound with the formula $Cu(NH(CH_3)_2)_2$(cyhdc) (Figure S26, Table S5), a stoichiometry consistent with that expected for the new phase formed after dimethylamine dosing. This phase crystallizes in the space group *C*2/*c*, and its structure is similar to that of $Cu(NH_2CH_3)_2$(cyhdc), featuring square planar copper centers bridged by cyhdc^{2-} linkers and coordinated by *trans* dimethylamines that engage in interchain hydrogen bonding interactions with nearby carboxylate oxygens (N−H···O = 2.02 Å). As noted above for $Cu(NH_2CH_3)_2$(cyhdc), it is possible that the lower symmetry phase accessed upon gas dosing features chains of the type $Cu(NH(CH_3)_2)_2$(cyhdc), but with a different crystal packing.

Under the conditions used here for single-crystal growth, we were not able to isolate the $Cu(NH_2CH_3)_4$(bdc) phase formed after dosing Cu(bdc) with 1 bar of monomethylamine. Instead, we obtained purple crystals of the intermediate $Cu(NH_2CH_3)_2$(bdc) phase (Figures 2b, S11 and S25) directly from a solution of copper(II), H_2bdc, and monomethylamine. This is also a one-dimensional compound with the formula $Cu(NH_2CH_3)_2$(bdc), as shown in Figure 4c, featuring square planar copper centers with a first coordination sphere analogous to that in $Cu(NH_2CH_3)_2$(cyhdc). Stabilizing interchain hydrogen bonding interactions ($d_{N-H\cdots O}$ = 2.08 and 2.19 Å) are evident between the amines and noncoordinated oxygen atoms of the carboxylate linkers.

Finally, we were able to identify the phase formed upon dosing Cu(bdc) with 1 bar of dimethylamine as the two-dimensional solid $Cu(NH(CH_3)_2)_2$(bdc) (Figure S27). This compound has been reported previously as the major product in the attempted synthesis of Cu(bdc) in dimethylformamide.[30] In this phase, chains of dicopper paddlewheel units are bridged by bidentate carboxylate linkers (d_{Cu-O} = 1.9905(14) Å), and additional linkers diagonally bridge copper ions in neighboring chains through coordination via a single oxygen (d_{Cu-O} = 2.2748(14) Å). One of the dimethylamines engages in hydrogen bonding interactions with the noncoordinated oxygen atom of the interchain linkers ($d_{N-H\cdots O}$ = 1.88 Å), such that the linkers are twisted with respect to neighbors in adjacent chains, and the adjacent aromatic rings engage in edge-to-face interactions. The second dimethylamine engages in hydrogen bonding with the bridging linker ($d_{N-H\cdots O}$ = 2.11 Å).

Ultimately, our single-crystal and powder X-ray diffraction data together suggest that methylamine uptake in Cu(cyhdc) and Cu(bdc) and the resulting structures formed are dictated by a complex interplay between the linker donor strength, amine donor strength, and number of hydrogen bond donors on the amine. It is interesting to consider these data together with the previously reported one-dimensional structure formed upon gaseous ammonia uptake in Cu(cyhdc).[24] We hypothesize that as the number of hydrogen bond donors decreases, and likewise as the linker donor strength decreases (e.g., moving from NH_3 to $NH(CH_3)_2$ and from cyhdc^{2-} to bdc^{2-}),

https://doi.org/10.1021/jacs.4c06718
J. Am. Chem. Soc. 2024, 146, 23943−23954

the formation of higher-dimensional amine-containing phases becomes increasingly favored, since this would maximize the stabilizing interactions in the resulting structure. Likewise, in the absence of stabilizing hydrogen bonding interactions, no structural change is expected to occur, as observed with trimethylamine uptake in Cu(cyhdc) and Cu(bdc). The fundamental drivers of such amine-induced phase changes are a topic under ongoing investigation in our laboratory.

Investigation of Tricomponent Methylamine Adsorption. The single-component methylamine adsorption data collected for Cu(cyhdc) and Cu(bdc) suggest that both materials may selectively capture monomethylamine over dimethylamine and trimethylamine over a range of pressures. Additionally, the distinct phase changes induced by monomethylamine and dimethylamine, in contrast to the physisorptive nature of trimethylamine uptake in both materials, are likely to subtly impact the selectivity of the materials for each gas. Considering this, we sought to investigate methylamine uptake in both frameworks under more realistic multicomponent conditions. However, owing to the toxicity and corrosivity of the amines, it was not possible to use breakthrough analysis. Instead, we dosed samples of each framework with gaseous mixtures of the three amines in $NH_2CH_3/NH(CH_3)_2/N(CH_3)_3$ molar ratios of 1:1:1, 2:1:1, 1:2:1, and 1:1:2 (with a total pressure of ~0.8 bar in each case), using a custom dosing manifold (see Figure S29 and the Experimental Section for details). After 1 day, a portion of each sample was digested and analyzed using ^{1}H NMR spectroscopy to quantify the amount of each amine adsorbed (Figure 5, Table S6), and powder X-ray diffraction analysis was used to characterize any structural phase changes (Figure S30). It should be noted that the actual ratio of the three gases in an industrial product stream is controlled by the catalyst and reaction conditions, and many ratios are possible.[3]

Proton NMR spectroscopy analysis of a digested sample of Cu(cyhdc) that had been dosed with a 1:1:1 ratio of the amines revealed the presence of NH_2CH_3 and $NH(CH_3)_2$ in approximately a 6:1 ratio (1.7 NH_2CH_3 per Cu versus 0.3 $NH(CH_3)_2$ per Cu), while no $N(CH_3)_3$ was detected (Figure 5a). Thus, Cu(cyhdc) is capable of selectively capturing monomethylamine over di- and trimethylamine under these conditions. The powder X-ray diffraction pattern for this sample featured reflections consistent with those characterized for the $P\bar{1}$ phase $Cu(NH_2CH_3)_2$(cyhdc) (Figure 3a), in addition to reflections from Cu(cyhdc) (Figure S30). Similar results were obtained when the framework was dosed with a 2:1:1 gas mixture (Figure 5a). Preferential uptake of monomethylamine (1.8 NH_2CH_3 per Cu) also occurred when Cu(cyhdc) was dosed with an excess of trimethylamine (a 1:1:2 mixture). In the diffraction pattern for the latter sample, the peaks associated with Cu(cyhdc) were more intense than those associated with $Cu(NH_2CH_3)_2$(cyhdc). Apparently then, even in the absence of a complete phase change, monomethylamine is preferentially adsorbed in the material.

Interestingly, a sample of Cu(cyhdc) dosed with the 1:2:1 mixture adsorbed similar amounts of mono- and dimethylamine—approximately 0.6 and 0.4 equiv, respectively, per copper site (Figure 5a), approximately half the expected uptake at the relevant partial pressure for each amine based on the single-component adsorption data (Figure 2a). The diffraction pattern for the resulting sample predominantly features reflections assignable to Cu(cyhdc), although low intensity

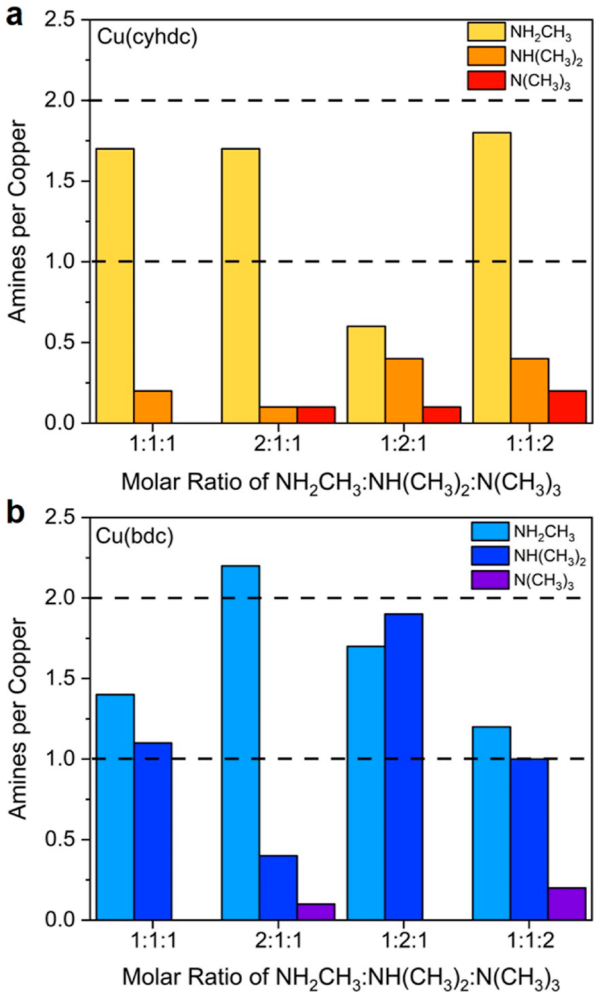

Figure 5. Amine loadings determined from ^{1}H NMR analysis of digested samples of (a) Cu(cyhdc) and (b) Cu(bdc) (Table S6) after exposure to varying ratios of mono-, di-, and trimethylamine using a custom-built gas dosing apparatus (see the Experimental Section for details). Framework samples were equilibrated with the amine mixture for 1 day before analysis. Powder X-ray diffraction patterns were also collected for each sample after equilibration (see Figure S30).

reflections are also apparent that could be assigned to $Cu(NH_2CH_3)_2$(cyhdc). Thus, under the conditions studied here, excess $NH(CH_3)_2$ can effectively compete with NH_2CH_3 for adsorption. Ultimately, these results indicate that over a range of mixed-gas dosing conditions, Cu(cyhdc) adsorbs significantly less trimethylamine than mono- and dimethylamine and is selective for monomethylamine for mixtures where it is present in an equimolar or excess amount relative to dimethylamine.

A sample of Cu(bdc) dosed with a 1:1:1 amine mixture adsorbed similar amounts of NH_2CH_3 and $NH(CH_3)_2$ (1.4 and 1.1 equiv per copper, respectively), and thus the material is not selective for monomethylamine under these conditions (Figure 5b). Interestingly, the powder X-ray diffraction pattern obtained for the resulting solid is distinct from patterns obtained for Cu(bdc), $Cu(NH_2CH_3)_2$(bdc), or $Cu(NH(CH_3)_2)_2$(bdc) (Figure S30). We sought to grow single crystals of this phase using a similar approach to that described for $Cu(NH_2CH_3)_2$(bdc), but using equimolar amounts of mono- and dimethylamine, although this did not yield a

https://doi.org/10.1021/jacs.4c06718
J. Am. Chem. Soc. 2024, 146, 23943−23954

structure consistent with the powder X-ray diffraction data (Figure S28). The same unknown phase was found to form upon dosing Cu(bdc) with a 1:2:1 mixture of the gases, and mono- and dimethylamine were adsorbed in similar amounts (1.7 and 1.9 equiv per copper site, respectively). However, when Cu(bdc) was dosed with a mixture containing excess trimethylamine (a 1:1:2 mixture), the resulting sample was amorphous, and analysis of the ^{1}H NMR spectrum of the digested sample revealed similar amounts of mono- and dimethylamine (1.2 and 1.0 equiv per copper, respectively) along with a small amount of trimethylamine (0.2 equiv per copper). In contrast, Cu(bdc) did exhibit selective uptake of monomethylamine when dosed with the 2:1:1 mixture of gases, capturing 2.2 equiv of NH_2CH_3 versus just 0.4 equiv of $NH(CH_3)_2$ per copper (a ∼6:1 ratio; Figure 5b). Powder X-ray diffraction analysis revealed that the resulting solid is amorphous (Figure S30).

In all, these results highlight that different compositions of the methylamine gas mixture can dramatically impact the uptake of the amines by both Cu(bdc) and Cu(cyhdc), and can promote or prevent the phase changes that occur under single-component adsorption conditions. While Cu(cyhdc) is capable of selectively capturing monomethylamine from a range of methylamine mixtures, the results for Cu(bdc) are more complex, although the framework is consistently selective for mono- and dimethylamine over trimethylamine. Considering these results, one could envision a separation scenario for a methylamine mixture where Cu(cyhdc) is first used to capture monomethylamine, and then Cu(bdc) is used to separate dimethylamine from the remaining mixture containing primarily di- and trimethylamine. Alternatively, Cu(bdc) could first be used to separate mono- and dimethylamine from trimethylamine, and then monomethylamine could be separated from dimethylamine using Cu(cyhdc).

CONCLUSIONS

In the foregoing work, we characterized the mono-, di-, and trimethylamine adsorption properties of the MOFs Cu(cyhdc) and Cu(bdc), toward the prospect of using these materials for methylamine separations. Gas adsorption data together with powder X-ray diffraction analysis of amine-dosed samples revealed that trimethylamine uptake occurs via physisorption in both frameworks, while uptake of mono- or dimethylamine triggers pressure- and temperature-dependent phase changes, reminiscent of the ammonia-induced phase change reported previously for Cu(cyhdc).[24] Consistent with the presence of a weaker carboxylate donor in Cu(bdc), the uptake of mono- or dimethylamine in Cu(bdc) is higher than in Cu(cyhdc) for a range of pressures. For example, dosing Cu(bdc) with 1 bar of monomethylamine results in the formation of a new phase featuring four amines per copper, while under the same conditions, Cu(cyhdc) adsorbs monomethylamine to form a phase featuring just two amines per copper site.

It was possible to structurally characterize some of the amine-containing phases using single-crystal X-ray diffraction analysis, which revealed that monomethylamine uptake in Cu(cyhdc) triggers formation of the one-dimensional solid $Cu(NH_2CH_3)_2$(cyhdc), featuring chains of square planar copper(II) centers bridged by cyhdc^{2-} linkers. The intermediate $Cu(NH_2CH_3)_2$(bdc) phase formed upon dosing Cu(bdc) with low pressures of monomethylamine adopts a similar structure. In contrast, dimethylamine uptake in Cu(bdc) results in the formation of the two-dimensional solid $Cu(NH(CH_3)_2)_2$(bdc)[30] with pyramidal copper centers. It is likely that the linker donor strength and availability of stabilizing hydrogen bonding interactions in the resulting structures are key drivers of the unique methylamine-induced phase changes characterized here. Finally, tricomponent adsorption data revealed that Cu(cyhdc) selectively adsorbs monomethylamine over di- and trimethylamine under a range of conditions. To the best of our knowledge, this study is the first to investigate the methylamine adsorption properties of MOFs, and it highlights the prospect of using these tunable adsorbents for especially challenging industrial separations. Ultimately, an in-depth analysis of the methylamine adsorption properties of these materials under more realistic conditions will be necessary to assess their true potential for methylamine separations.

EXPERIMENTAL SECTION

General. All reagents were purchased from commercial vendors and used as received. Ultrahigh-purity-grade (99.999%) He, N_2, and Ar and anhydrous (99.9%) mono-, di-, and trimethylamine were used for gas adsorption measurements. Solutions of monomethylamine in methanol (10.0 M) and dimethylamine in methanol or ethanol (2.0 M) were purchased from TCI Chemicals and used as received. Note: the methylamines are toxic, corrosive, and flammable, and they should only be handled in a fume hood with at least 100 fpm of ventilation, using only compatible materials such as 316 stainless steel and Kalrez or EPDM o-rings. Proper respirator protection is also recommended. All these precautions were used in the present work. The compounds Cu(cyhdc) and Cu(bdc) were prepared under ambient conditions using as-received solvents (see below). Attenuated total reflectance infrared spectra were collected on a PerkinElmer Spectrum 400 Fourier transform IR spectrometer on the benchtop under air.

Cu(cyhdc) Synthesis. The MOF Cu(cyhdc) was prepared by slightly modifying the procedure reported in ref 24. In brief, the temperature used for solvothermal synthesis used in the current work was slightly higher, and the activation temperature used in the current work was slightly lower, than in ref 24; these changes were found to yield a material with optimal surface area. A 100 mL bottle was charged with $Cu(NO_3)_2{\cdot}2.5H_2O$ (1.163 g, 5.000 mmol), *trans*-1,4-cyclohexanedicarboxylic acid (0.861 g, 5.00 mmol), *N*,*N*-dimethylformamide (DMF; 50 mL), and the mixture was bath sonicated at room temperature until the solids dissolved. The resulting blue solution was then heated for 24 h in an oven held at 100 °C. After the mixture had been cooled to room temperature, a teal precipitate was isolated by vacuum filtration and rinsed with DMF heated to 80 °C (15 mL × 4). The precipitate was subsequently rinsed with methanol (15 mL × 4), soaked in 50 mL methanol for 24 h, and then stored in 50 mL fresh methanol. Cu(cyhdc) was activated as follows: the framework was vacuum filtered to remove the methanol supernatant, and then transferred to a Schlenk flask. The flask was held under vacuum on a Schlenk line at 25 °C for 30 min, and then using a sand bath, the temperature was increased to 120 °C and the sample was held at this temperature under vacuum for 18 h. The teal solid did not change color upon activation (0.831 g, 71.1%). Elemental analysis: % calc. for $CuC_8O_4H_{10}$: C 41.1, H 4.3; % found: C 40.7, H 4.3, Cu and O unmeasured.

Cu(bdc) Synthesis. The MOF Cu(bdc) was synthesized following the same procedure described above for Cu(cyhdc), but with terephthalic acid (0.834 g, 5.00 mmol) as the linker.[29] After initial synthesis, the precipitate was a light blue. The resulting material was activated as follows: the framework was vacuum filtered to remove the methanol supernatant, and then transferred to a Schlenk flask. The flask was held under vacuum on a Schlenk line at 25 °C for 30 min, and then using a sand bath, the temperature was increased to 120 °C and the sample was held at this temperature under vacuum for 18 h. The activated material is dark blue (0.740 g, 65.0%). Elemental analysis: % calc. for $CuC_8O_4H_{10}$: C 42.2, H 1.8; % found: C 41.8, H 1.8, Cu and O unmeasured.

https://doi.org/10.1021/jacs.4c06718
J. Am. Chem. Soc. 2024, 146, 23943−23954

Proton NMR Analysis of Digested Samples. Proton NMR spectra were collected using a NEO AV-500 spectrometer at ambient temperature, and all chemical shifts are reported in relation to residual solvent peaks. Approximately 2 mg of a given sample was dissolved in 1 mL of methanol-d_4 or THF-d_8, and then ∼5 drops of 1 M DCl in D_2O were added to the solution to dissolve all solids. Ratios of amine to copper sites reported in the text were determined by comparing the integration values for the linker proton peaks to the methylamine protons peak(s). The ratio of linker to copper in Cu(cyhdc) and Cu(bdc) is one to one, so the amine loading relative to the linker was assumed to be the same as the loading relative to each copper ion.

Thermogravimetric Analysis. Thermogravimetric analyses were performed using a TA Instruments Discovery thermogravimetric analyzer. Decomposition experiments were carried out under dry N_2 using a flow rate of 10 or 25 mL/min (ramp rate of 1 °C/min). Approximately 10 mg of Cu(cyhdc), Cu(bdc), or amine-dosed samples of the frameworks (see "Preparation of Gas-Dosed Samples" below) were placed in an aluminum pan and immediately loaded into the oven. Desorption temperatures were estimated from the point inflection after initial mass loss. Loadings in amines per copper were calculated using eq 1 and the masses before and after the mass loss region.

$$\text{Loading} = \frac{m_{\text{final}} - m_{\text{initial}}}{\text{MW}_{\text{methylamine}}} \times \frac{\text{MW}_{\text{MOF}}}{m_{\text{final}}} \quad (1)$$

Single-Component Gas Adsorption and Desorption Isotherms. Samples of activated framework (approximately 50−100 mg) were transferred to preweighed glass analysis tubes, then capped with TranSeals sealed with Viton o-rings for N_2 adsorption or EPDM o-rings for the methylamine gases. Gas sorption isotherms were collected using Micromeritics ASAP2420 or 3Flex analyzers. Oil-free vacuum pumps and pressure regulators were used for all measurements to prevent contamination of the samples and the gases. Prior to isotherm collection, the samples were heated from 25 to 120 °C at a ramp rate of 2 °C/min, and then held at 120 °C and holding until an outgas rate of less than 2 μbar/min was achieved (approximately 4 h). The evacuated analysis tube containing the activated sample was then reweighed to determine an accurate starting sample mass. Isothermal amine adsorption data were collected between 10 and 100 °C. Sample temperatures were maintained with a Julabo Corio CD-200F refrigerated/heating circulator. Nitrogen adsorption isotherms collected at 77 K were measured using a liquid nitrogen bath, and Brunauer−Emmett−Teller and Langmuir surface areas were calculated from the isothermal data.

The isothermal adsorption and desorption data were collected using software produced by Micromeritics. As defined by the software, equilibration at each pressure was achieved when the pressure change in the headspace for a given equilibration interval was less than 0.01% of the average pressure during the interval. For the methylamine (N_2) adsorption and desorption data collection, the headspace pressure was measured every 30 s (15 s), and the software automatically compared the change in the pressure across 11 of these 30 s (15 s) increments. If equilibration was not achieved during the first 5.5 min (2.75 min) interval, additional data points were taken in 30 s (15 s) intervals, until a change of 0.01% or less in the pressure was measured; the last pressure corresponding to the data set meeting this criterion was recorded as the pressure and used to determine the amine loading. Each point on the methylamine isotherms took a different total time for collection; points within regions of steep uptake took as long as ∼18 h to equilibrate, while other points equilibrated within as little as 1 h.

Preparation of Gas-Dosed Samples. Gas-dosed samples used for powder X-ray diffraction experiments, Fourier transform IR spectroscopy, or thermogravimetric analysis were prepared as follows. The compounds Cu(cyhdc) or Cu(bdc) were activated in a glass analysis tube at 120 °C until an outgas rate of less than 2 μbar/min was achieved. The activated samples were then connected to a Micromeritics 3Flex, placed under vacuum, and submerged in an oil bath held at 10 or 25 °C by a Julabo Corio CD-200F refrigerated/heating circulator. This temperature was maintained for the entirety of the dosing experiment. The sample tube was then dosed with the desired pressure of mono-, di-, or trimethylamine for 30 s. The sample port was closed after dosing, and any subsequent pressure drop was monitored using the 3Flex instrument. For samples dosed with mono- or dimethylamine pressures less than 1 bar, the frameworks were dosed only once and then left to equilibrate under the static pressure for 1 day. Typically, a pressure drop of ∼0.1 to 0.2 bar occurred during this time, depending on the initial dosed pressure. The final equilibrated pressures are those reported in Figures S8 and S9 and discussed in the text, corresponding to various pressures before, within, or after the regions of steep uptake in the corresponding adsorption isotherms. For each sample dosed with 1 bar of gas, a significant pressure drop occurred within 5 min, and after 15 min, the sample port was opened, and the sample was dosed again with 1 bar of gas. The material was then left to equilibrate under this static pressure for one or more days. After dosing, all samples were brought into a N_2 glovebox and transferred to a 20 mL vial for handling and storage.

Powder X-ray Diffraction Analysis. Samples of the activated frameworks or frameworks dosed ex situ with methylamine gas (see "Preparation of Gas-Dosed Samples") were loaded into 1.0 mm boron-rich glass capillaries inside a N_2 glovebox (∼5 mg in each case). The capillary opening was sealed with silicone grease, and then the capillary was taken out of the box and sealed immediately using the flame of a small tea light candle. Additional portions of these samples were set aside for digestion and ^{1}H NMR spectroscopy analysis to determine amine loading.

Laboratory powder X-ray diffraction data were collected on a Bruker AXS D8 Advanced diffractometer equipped with a Cu K_α source (λ = 1.54 Å) and a zero-background silicon holder (Figures S10, S11, S14, S15, S17, S19, S21, S23, and S30). High-resolution synchrotron X-ray powder diffraction data were also collected for ex situ dosed samples at Beamline 17-BM at the Advanced Photon Source at Argonne National Laboratory (λ = 0.45171 Å), which is equipped with a PerkinElmer a-Si flat panel detector and an Oxford Cryosystems Cryostream; or at Beamline 28-ID-2 at the National Synchrotron Light Source II at Brookhaven National Laboratory (λ = 0.1814 Å), which is equipped with a CsI-coated flat scintillator panel and an Oxford Cryosystems Cryostream (Figures 3, S1, S9, S12, S13, S24, and S25).

Powder X-ray diffraction data collected for amine-dosed samples with heating under N_2 were also collected at Beamline 28-ID-2 using a gas flow capillary reactor. For these experiments, samples dosed ex situ with methylamine were packed into polyimide tubes (inner diameter of 0.0578″ and outer diameter of 0.0615″) between two pieces of glass wool. The tube was loaded into a cell provided by the beamline and connected to a mass flow controller with 10 mL/min of 99.999% N_2 gas flowing into the cell. An Oxford Cryosystems Cryostream was positioned above the sample to heat from 25 to 200 °C at 5 °C/min. Powder X-ray diffraction patterns were collected for samples every minute (Figures S11 and S12).

The powder X-ray diffraction data are reported in units of $Q = 4\pi \cdot \sin(\theta)/\lambda$ (Q is the scattering vector)[31] to allow for comparisons between data collected with different wavelengths. Structure analyses, including indexing and Pawley refinements, were performed with the program TOPAS-Academic v6.

Crystallization of Methylamine-Containing Phases. Single crystals of amine-containing phases were generally grown by combining a solution of copper(II) triflate dissolved in DMF with a solution of the linker and amine of interest. Solutions of 2.0 M monomethylamine in methanol or 2.0 M dimethylamine in methanol or ethanol were used as specified. Vapor diffusion of DMF into this mixture at room temperature yielded crystals of the phases discussed in the text.

Cu(NH_2CH_3)$_2$(cyhdc). Solid H_2cyhdc (4.3 mg, 0.025 mmol) was added to a 2.0 M solution of NH_2CH_3 in methanol (0.50 mL), and this mixture was combined with a solution of $Cu(CF_3SO_3)_2$ (7.3 mg, 0.020 mmol) in DMF (0.50 mL). The solutions were mixed in an open 2 mL vial to give copper(II), H_2cyhdc, and NH_2CH_3 in a

https://doi.org/10.1021/jacs.4c06718
J. Am. Chem. Soc. 2024, 146, 23943−23954

1.0:1.3:50 molar ratio. This vial was then placed in a closed 20 mL vial containing approximately 3 mL of DMF. After 1 day, purple plate crystals formed.

$Cu(NH(CH_3)_2)_2(cyhdc)$. Solid H_2cyhdc (4.3 mg, 0.025 mmol) was added to a 2.0 M solution of $NH(CH_3)_2$ in methanol (0.50 mL), and this mixture was combined with a solution of $Cu(CF_3SO_3)_2$ (6.9 mg, 0.019 mmol) in DMF (0.50 mL). The solutions were mixed in an open 2 mL vial to give copper(II), H_2cyhdc, and $NH(CH_3)_2$ in a 1.0:1.3:53 molar ratio. This vial was then placed in a closed 20 mL vial containing approximately 3 mL of DMF. After 1 day, blue plate crystals formed.

$Cu(NH_2CH_3)_2(bdc)$. Solid H_2bdc (8.3 mg, 0.050 mmol) was added to a 2.0 M solution of NH_2CH_3 in methanol (0.50 mL), and this mixture was combined with a solution of $Cu(CF_3SO_3)_2$ (9.0 mg, 0.025 mmol) in DMF (0.50 mL). The solutions were mixed in an open 2 mL vial to give copper(II), H_2bdc, and NH_2CH_3 in a 1.0:2.0:40 molar ratio. This vial was then placed in a closed 20 mL vial containing approximately 3 mL of DMF. After 1 day, purple plate crystals formed.

$Cu(NH(CH_3)_2)_2(bdc)$. Solid H_2bdc (8.3 mg, 0.050 mmol) was added to a 2.0 M solution of $NH(CH_3)_2$ in methanol (0.50 mL), and this mixture was combined with a solution of $Cu(CF_3SO_3)_2$ (4.5 mg, 0.013 mmol) in 2.0 M $NH(CH_3)_2$ in ethanol (0.50 mL). The solutions were mixed in an open 2 mL vial to give copper(II), H_2cyhdc, and NH_2CH_3 in a 1.0:4.0:160 molar ratio. This vial was then placed in a closed 20 mL vial containing approximately 3 mL of DMF. After 1 day, blue needle crystals formed.

$Cu(NH_2CH_3)(NH(CH_3)_2)(bdc)\cdot DMF$. Solid H_2bdc (8.3 mg, 0.050 mmol) was added to a solution of 1.0 M NH_2CH_3 and 1.0 M $NH(CH_3)_2$ in methanol (0.50 mL), and this mixture was combined with a solution of $Cu(CF_3SO_3)_2$ (4.5 mg, 0.013 mmol) in DMF (0.50 mL). The solutions were mixed in an open 2 mL vial to give copper(II), H_2bdc, NH_2CH_3, and $NH(CH_3)_2$ in a 1.0:4.0:40:40 molar ratio. This vial was then placed in a closed 20 mL vial containing approximately 3 mL of DMF. After 1 day, purple block crystals formed.

Single-Crystal X-ray Diffraction Analysis. Single crystal X-ray diffraction data were collected on single crystals coated with Paratone-N oil and mounted on MiTeGen loops. The crystals were frozen at 100(2) K by an Oxford Cryosystems Cryostream 700. Data for $Cu(NH_2CH_3)_2(bdc)$ and $Cu(NH(CH_3)_2)_2(bdc)$ were collected at the UC Berkeley CHEXRAY crystallographic facility on a Rigaku XtaLAB P200 equipped with a MicroMax 007HF rotating anode and a Pilatus 200 K hybrid pixel array detector using Cu Kα radiation (λ = 1.5418 Å) or Mo Kα radiation (λ = 0.71073 Å). Data collection, processing, and reduction were performed with CrysAlisPro. Data for $Cu(NH_2CH_3)_2(cyhdc)$, $Cu(NH(CH_3)_2)_2(cyhdc)$, and $Cu(NH_2CH_3)(NH(CH_3)_2)(bdc)\cdot DMF$ were collected at the Advanced Light Source Station 12.2.1, Lawrence Berkeley National Laboratory. The data were collected using synchrotron radiation (λ = 0.7288 Å) and a Bruker AXS D8 diffractometer with a Bruker PHOTON II CMOS detector. The Bruker AXS SAINT software was used to correct for Lorentz and polarization effects. SADABS was used for absorption corrections. The structures were solved by intrinsic phasing with SHELXT and refined using SHELXL operated in the OLEX2 interface (see Table S5). Thermal parameters were refined anisotropically for all non-hydrogen atoms. Hydrogen positions were included at the geometrically calculated positions and refined using a riding model.

Amine Desorption and Regeneration of Amine-Containing Phases. Approximately 50 mg of Cu(cyhdc) or Cu(bdc) were activated in a glass analysis tube at 120 °C until an outgas rate of less than 2 μbar/min was achieved. The samples were then dosed with 1 bar of mono- or dimethylamine at 10 or 25 °C on a Micromeritics 3Flex (see "Preparation of Gas-Dosed Samples"). About 5 mg of the sample were then sealed in a glass capillary for powder X-ray diffraction analysis. The resulting data are presented in Figures S14 and S15. Another ∼2 mg of each sample was digested with acid and analyzed using ^{1}H NMR spectroscopy (see "Proton NMR Analysis of Digested Samples").

Separately, approximately 20 mg of each amine-dosed sample was placed into an aluminum pan and immediately loaded into the oven of a TA Instruments Discovery Thermogravimetric Analyzer. The samples were first heated from 25 to 180 °C under flowing dry N_2 (flow rate of 10 mL/min, temperature ramp rate of 1 °C/min), and then the samples were held at 180 °C for 1 h under flowing N_2. The activated samples were analyzed using powder X-ray diffraction and, and the resulting data are also reported in Figures S14 and S15. A portion of each activated sample (∼5 mg) was digested with acid and analyzed using proton NMR spectroscopy. The remaining ∼15 mg of each activated sample was transferred to a glass analysis tube and evacuated at 120 °C on a Micromeritics 3Flex until an outgas rate of less than 2 μbar/min was achieved. The samples were then dosed again with 1 bar of mono- or dimethylamine at 10 or 25 °C, as described above, and the equilibrated samples were analyzed using powder X-ray diffraction (see Figures S14 and S15).

Amine Adsorption−Desorption Cycling. Approximately 10 mg of Cu(cyhdc) or Cu(bdc) were activated in a glass analysis tube at 120 °C until an outgas rate of less than 2 μbar/min was achieved. The sample was then transferred to an aluminum pan for the thermogravimetric analysis instrument and placed in a 20 mL vial. The vial was connected to the custom-build apparatus illustrated in Figure S29. The sample was evacuated and then dosed with 1 bar of mono- or dimethylamine at 10 or 25 °C using this apparatus. The temperature was maintained using a Julabo Corio CD-200F refrigerated/heating circulator. For each adsorption run, samples of Cu(cyhdc) and Cu(bdc) were dosed with monomethylamine at 25 °C and allowed to equilibrate for 30 min, a sample of Cu(cyhdc) was dosed with dimethylamine at 10 °C and allowed to equilibrate for 1 d, and a sample of Cu(bdc) was dosed with dimethylamine at 25 °C and allowed to equilibrate for 30 min. Following adsorption, each sample was transferred to the thermogravimetric analyzer for desorption. During transfer, the aluminum pan was exposed to air for less than 60 s, and no color change was noted during the transfer for any material. Under a flow of N_2 (25 mL/min), the amine-dosed samples were then heated from ambient temperature to 180 or 200 °C at a rate of 1 °C/min and then held isothermally for 30 and 60 min for Cu(cyhdc) and Cu(bdc), respectively. The temperature of each sample was then ramped down to 25 °C at 25 °C/min. The aluminum pan was then transferred back to a 20 mL vial and evacuated at ambient temperature for 15 min to remove air from the system. This adsorption−desorption cycling procedure was repeated for a total of five cycles on the same sample. The thermogravimetric analysis results are shown in Figures S16, S18, S20, and S22 in the Supporting Information, normalized to the mass at the end of the experiment to account for small mass losses during sample transfer. After the fifth cycle of each experiment, a portion of the sample was transferred to a glass capillary and sealed. The remaining sample was evacuated for 15 min, dosed with 1 bar of the corresponding amine at 10 or 25 °C, then transferred to a capillary and sealed for powder X-ray diffraction analysis (Figures S17, S19, S21, and S33).

Tricomponent Adsorption Analysis. Approximately 50 mg of Cu(cyhdc) or Cu(bdc) were activated in a glass analysis tube at 120 °C until an outgas rate of less than 2 μbar/min was achieved. The frameworks were then dosed with mixtures of the three amines using a custom-build apparatus illustrated in Figure S29. All experiments were conducted at room temperature. The apparatus manifold consists of 316 stainless steel tubes connecting four needle valves to a central four-way connector. The first needle valve connects to the glass analysis tube containing the sample through a 316 stainless steel tube and an adapter provided by Micromeritics. The second valve connects to a vacuum pump through rubber tubing. The third valve connects to an MKS pressure transducer with a range of 0 to 6 bar through a 316 stainless steel tube. The fourth valve connects to a custom-build gas mixing chamber. The mixing chamber consists of three 50 mL, 316 stainless steel, double-ended cylinders connected in series through ball valves that can be set to open or closed. These ball valves are used to isolate the three cylinders from each other. Each 50 mL cylinder is directly connected to a pure gas cylinder through a 316 stainless steel

https://doi.org/10.1021/jacs.4c06718
J. Am. Chem. Soc. 2024, 146, 23943−23954

tube, allowing for the 50 mL cylinder to be filled to a desired pressure with pure gas.

Prior to each dosing experiment, the entire custom-build manifold, including the sample in the glass analysis tube, the pressure transducer, and the three 50 mL cylinders, were evacuated to 20 mTorr. Then, the needle valve connected to the gas mixing chamber was closed to isolate it from vacuum. The ball valves between each of the three 50 mL cylinders were closed, and each cylinder was pressurized to a recorded pressure. For a molar ratio of 1:1:1 of mono-to di-to trimethylamine, each cylinder was pressurized to 30 psi. For a ratio of 2:1:1, the monomethylamine chamber was pressurized to 30 psi, while the di- and trimethylamine chambers were pressurized to 15 psi. The 1:2:1 and 1:1:2 ratios were made with dimethylamine and trimethylamine at 30 psi respectively, with the other two gases pressurized to 15 psi. After the three 50 mL cylinders were pressurized, the pure gas cylinders were closed, and the ball valves separating the 50 mL cylinders were opened. The gases were allowed to mix for 24 h under static conditions. After this mixing period, the vacuum connection was closed, and the needle valve connecting to the gas mixing chamber was opened to pressurize the manifold and glass sample analysis tube to 1.0 bar, as read through the pressure transducer. The final pressure of the sample after 15 min of equilibration was approximately 0.8 bar for each sample tested. Each sample was allowed to equilibrate at room temperature for 24 h and then brought into a N_2 glovebox for sampling and handling. About 5 mg of each sample was sealed into glass capillaries for powder X-ray diffraction analysis using the laboratory equipment. About 2 mg of each sample was digested with acid and analyzed using proton NMR spectroscopy (see "Proton NMR Analysis of Digested Samples").

■ ASSOCIATED CONTENT

Supporting Information

The Supporting Information is available free of charge at https://pubs.acs.org/doi/10.1021/jacs.4c06718.

Additional experimental characterization data, X-ray crystallography data, and single and tricomponent adsorption data (PDF)

Accession Codes

CCDC 2326862, 2326863, 2326864, 2326865, 2326866 contain the Supporting Information crystallographic data for this paper. These data can be obtained free of charge via www.ccdc.cam.ac.uk/data_request/cif, or by emailing data_request@ccdc.cam.ac.uk, or by contacting The Cambridge Crystallographic Data Centre, 12 Union Road, Cambridge CB2 1EZ, UK; fax: +44 1223 336033.

■ AUTHOR INFORMATION

Corresponding Author

Jeffrey R. Long − *Institute for Decarbonization Materials, Department of Chemistry, and Department of Chemical and Biomolecular Engineering, University of California, Berkeley, California 94720, United States; Department of Materials Science and Engineering, University of California, Berkeley, California 94720, United States; Materials Sciences Division, Lawrence Berkeley National Laboratory, Berkeley, California 94720, United States;* orcid.org/0000-0002-5324-1321; Email: jrlong@berkeley.edu

Authors

Katerina I. Graf − *Institute for Decarbonization Materials and Department of Chemistry, University of California, Berkeley, California 94720, United States; Materials Sciences Division, Lawrence Berkeley National Laboratory, Berkeley, California 94720, United States;* orcid.org/0000-0003-3584-7861

Adrian J. Huang − *Institute for Decarbonization Materials and Department of Chemistry, University of California, Berkeley, California 94720, United States; Materials Sciences Division, Lawrence Berkeley National Laboratory, Berkeley, California 94720, United States*

Katie R. Meihaus − *Institute for Decarbonization Materials and Department of Chemistry, University of California, Berkeley, California 94720, United States*

Complete contact information is available at: https://pubs.acs.org/10.1021/jacs.4c06718

Author Contributions

The manuscript was written through contributions of all authors. All authors have given approval to the final version of the manuscript.

Notes

The authors declare no competing financial interest.

■ ACKNOWLEDGMENTS

This research was supported by the U.S. Department of Energy, Office of Basic Energy Sciences, Separation Science in the Chemical Sciences, Geosciences, and Biosciences Division, under award number DE-SC0019992. Some of the powder X-ray diffraction data were collected at Beamline 17-BM-B at the Advanced Photon Source, a DOE Office of Science User Facility, operated by Argonne National Laboratory under contract DE-AC02-06CH1135. This research used resources of the National Synchrotron Light Source II, Beamline 28-ID-2, a U.S. Department of Energy (DOE) Office of Science User Facility operated for the DOE Office of Science by Brookhaven National Laboratory under Contract no. DE-SC0012704. This research used resources of the Advanced Light Source, Beamline 12.2.1, a U.S. DOE Office of Science User Facility under Contract no. DE-AC02-05CH11231. We thank Dr. Benjamin Snyder for helpful discussions regarding materials synthesis and cooperative adsorption. We are grateful to Dr. Maria Paley, Dr. Malia Wenny, and Dr. Ryan Klein for guidance on powder X-ray diffraction analysis. We thank Dr. Ever Velasquez for assistance with isothermal measurements.

■ REFERENCES

(1) Sholl, D. S.; Lively, R. P. Seven Chemical Separations to Change the World. *Nature* **2016**, *532* (7600), 435−437.

(2) Angelini, P.; Armstrong, T.; Counce, R.; Griffith, W.; Klasson, T.; Muralidharan, G.; Narula, C.; Sikka, V.; Closset, G.; Keller, G.; Watson, J. *Materials for Separation Technologies. Energy and Emission Reduction Opportunities*; Oak Ridge National Laboratory: Oak Ridge, TN, 2005.

(3) Roose, P. Methylamines. In *Ullmann's Encyclopedia of Industrial Chemistry*; Wiley-VCH Verlag GmbH & Co. KGaA: Weinheim, Germany, 2015; pp 1−10.

(4) Corbin, D. R.; Schwarz, S.; Sonnichsen, G. C. Methylamines Synthesis: A Review. *Catal. Today* **1997**, *37* (2), 71−102.

(5) Cook, D.; Young, D. M. Process for Separating Methylamines. U.S. Patent 3,271,455 A, 1966.

(6) Duranleau, R. G.; Zimmerman, R. Amine Separation Process. U.S. Patent 5,189,221 A, 1993.

(7) Binau, D.; Speicher, E. Methylamines Purification by Distillation and Purge. U.S. Patent 4,283,254 A, 1981.

(8) Andrews, C.; Spence, L. R. Process for Separation and Purification of Methyl Amines. U.S. Patent 2,061,889 A, 1936.

(9) Spence, L. R. Process for the Separation of Trimethylamine From Mixtures of Trimethylamine and Dimethylamine. U.S. Patent 2,206,585 A, 1940.

(10) Gao, K.; Wang, Q.; Du, X.; Wei, Q.; Huang, Y. Efficient Adsorption and Eco-Environmental Oxidization of Dimethylamine in Beta Zeolite. *Microporous Mesoporous Mater.* **2019**, *282*, 219−227.
(11) Liu, Z.; Yin, Z.; Zhang, Z.; Gao, C.; Yang, Z.; Yang, W. Removal of Aliphatic Amines by NiLa-Layered Double Hydroxide Nanostructures. *ACS Appl. Nano Mater.* **2022**, *5* (6), 8120−8130.
(12) Cook, W. G.; Ross, R. A. Heterogeneous Interactions of Methylamines on Porous Adsorbents. Part I. The Adsorption of Monomethylamine on Silica Gels and Silica-Alumina. *Can. J. Chem.* **1972**, *50* (11), 1666−1674.
(13) Cook, W. G.; Ross, R. A. Heterogeneous Interactions of Methylamines on Porous Adsorbents Part II. Interactions on Silica-Alumina and Silica Gel Surfaces of Di- and Tri-Methylamine in the Region of Their Boiling Points. *Can. J. Chem.* **1972**, *50* (15), 2451−2456.
(14) Kökçam-Demir, Ü.; Goldman, A.; Esrafili, L.; Gharib, M.; Morsali, A.; Weingart, O.; Janiak, C. Coordinatively Unsaturated Metal Sites (Open Metal Sites) in Metal-Organic Frameworks: Design and Applications. *Chem. Soc. Rev.* **2020**, *49* (9), 2751−2798.
(15) Li, J.; Jiang, L.; Chen, S.; Kirchon, A.; Li, B.; Li, Y.; Zhou, H.-C. Metal-Organic Framework Containing Planar Metal-Binding Sites: Efficiently and Cost-Effectively Enhancing the Kinetic Separation of C_2H_2/C_2H_4. *J. Am. Chem. Soc.* **2019**, *141* (9), 3807−3811.
(16) Wang, H.; Liu, Y.; Li, J. Designer Metal-Organic Frameworks for Size-Exclusion-Based Hydrocarbon Separations: Progress and Challenges. *Adv. Mater.* **2020**, *32* (44), 2002603.
(17) Hu, Z.; Wang, Y.; Farooq, S.; Zhao, D. A Highly Stable Metal-Organic Framework with Optimum Aperture Size for CO_2 Capture. *AIChE J.* **2017**, *63* (9), 4103−4114.
(18) McDonald, T. M.; Mason, J. A.; Kong, X.; Bloch, E. D.; Gygi, D.; Dani, A.; Crocellà, V.; Giordanino, F.; Odoh, S. O.; Drisdell, W. S.; Vlaisavljevich, B.; Dzubak, A. L.; Poloni, R.; Schnell, S. K.; Planas, N.; Lee, K.; Pascal, T.; Wan, L. F.; Prendergast, D.; Neaton, J. B.; Smit, B.; Kortright, J. B.; Gagliardi, L.; Bordiga, S.; Reimer, J. A.; Long, J. R. Cooperative Insertion of CO_2 in Diamine-Appended Metal-Organic Frameworks. *Nature* **2015**, *519* (7543), 303−308.
(19) Mellot-Draznieks, C.; Serre, C.; Surblé, S.; Audebrand, N.; Férey, G. Very Large Swelling in Hybrid Frameworks: A Combined Computational and Powder Diffraction Study. *J. Am. Chem. Soc.* **2005**, *127* (46), 16273−16278.
(20) Shivanna, M.; Yang, Q.-Y.; Bajpai, A.; Patyk-Kazmierczak, E.; Zaworotko, M. A Dynamic and Multi-Responsive Porous Flexible Metal-Organic Material. *Nat. Commun.* **2018**, *9* (1), 3080.
(21) Rosenbach, N., Jr.; Ghoufi, A.; Déroche, I.; Llewellyn, P.; Devic, T.; Bourrelly, S.; Serre, C.; Férey, G.; Maurin, G. Adsorption of Light Hydrocarbons in the Flexible MIL-53(Cr) and Rigid MIL-47(V) Metal-Organic Frameworks: A Combination of Molecular Simulations and Microcalorimetry/Gravimetry Measurements. *Phys. Chem. Chem. Phys.* **2010**, *12* (24), 6428−6437.
(22) Kumagai, H.; Akita-Tanaka, M.; Inoue, K.; Takahashi, K.; Kobayashi, H.; Vilminot, S.; Kurmoo, M. Metal-Organic Frameworks from Copper Dimers with *Cis*- and *Trans*-1,4-Cyclohexanedicarboxylate and *Cis,Cis*-1,3,5-Cyclohexanetricarboxylate. *Inorg. Chem.* **2007**, *46* (15), 5949−5956.
(23) Seki, K.; Takamizawa, S.; Mori, W. Characterization of Microporous Copper(II) Dicarboxylates (Fumarate, Terephthalate, and *Trans*-1,4-Cyclohexanedicarboxylate) by Gas Adsorption. *Chem. Lett.* **2001**, *30* (2), 122−123.
(24) Snyder, B. E. R.; Turkiewicz, A. B.; Furukawa, H.; Paley, M. V.; Velasquez, E. O.; Dods, M. N.; Long, J. R. A Ligand Insertion Mechanism for Cooperative NH_3 Capture in Metal-Organic Frameworks. *Nature* **2023**, *613* (7943), 287−291.
(25) Chen, Y.; Du, Y.; Liu, P.; Yang, J.; Li, L.; Li, J. Removal of Ammonia Emissions via Reversible Structural Transformation in M(BDC) (M = Cu, Zn, Cd) Metal-Organic Frameworks. *Environ. Sci. Technol.* **2020**, *54* (6), 3636−3642.
(26) Lyu, P.; Wright, A. M.; López-Olvera, A.; Mileo, P. G. M.; Zárate, J. A.; Martínez-Ahumada, E.; Martis, V.; Williams, D. R.; Dincă, M.; Ibarra, I. A.; Maurin, G. Ammonia Capture via an Unconventional Reversible Guest-Induced Metal-Linker Bond Dynamics in a Highly Stable Metal-Organic Framework. *Chem. Mater.* **2021**, *33* (15), 6186−6192.
(27) Paul, B.; Zimmermann, B.; Fromm, K. M.; Janiak, C. [M(μ-O_2C-C_6H_4-CO_2)$(NH_3)_2$] (M = Cu, Cd; O_2C-C_6H_4-CO_2 = Benzene-1, 4-Dicarboxylate, Terephthalate): 1D Coordination Polymers with Strong Inter-Chain Hydrogen Bonding. *Z. Für Anorg. Allg. Chem.* **2004**, *630* (11), 1650−1654.
(28) Carson, C. G.; Hardcastle, K.; Schwartz, J.; Liu, X.; Hoffmann, C.; Gerhardt, R. A.; Tannenbaum, R. Synthesis and Structure Characterization of Copper Terephthalate Metal-Organic Frameworks. *Eur. J. Inorg. Chem.* **2009**, *2009* (16), 2338−2343.
(29) Carson, C. G.; Brunnello, G.; Lee, S. G.; Jang, S. S.; Gerhardt, R. A.; Tannenbaum, R. Structure Solution from Powder Diffraction of Copper 1,4-Benzenedicarboxylate. *Eur. J. Inorg. Chem.* **2014**, *2014* (12), 2140−2145.
(30) Hawxwell, S. M.; Brammer, L. Solvent Hydrolysis Leads to an Unusual Cu(II) Metal-Organic Framework. *CrystEngComm* **2006**, *8* (6), 473.
(31) Girolami, G. S. *X-Ray Crystallography*; University Science Books: Mill Valley, CA, 2016.

https://doi.org/10.1021/jacs.4c06718
J. Am. Chem. Soc. 2024, 146, 23943−23954